

Article

Methodology for Phytoplankton Taxonomic Group Identification towards the Development of a Lab-on-a-Chip

Denise A. M. Carvalho ¹, Vânia C. Pinto ^{1,2,*}, Paulo J. Sousa ^{1,2}, Vitor H. Magalhães ¹, Emilio Fernández ³, Pedro A. Gomes ⁴, Graça Minas ^{1,2,*} and Luís M. Gonçalves ^{1,2}

- ¹ Center for MicroElectromechanical Systems (CMEMS-UMinho), University of Minho, 4800-058 Guimarães, Portugal; id6815@alunos.uminho.pt (D.A.M.C.); psousa@dei.uminho.pt (P.J.S.); vvhvm@live.com.pt (V.H.M.); lgoncalves@dei.uminho.pt (L.M.G.)
- ² LABBELS—Associate Laboratory, Braga/Guimarães, Portugal
- ³ Grupo de Oceanografía Biológica, Faculty of Marine Science, Universidade de Vigo, 36310 Pontevedra, Spain; esuarez@uvigo.es
- ⁴ CBMA—Molecular and Environmental Biology Centre, University of Minho, Campus de Gualtar, 4710-074 Braga, Portugal; pagomes@bio.uminho.pt
- * Correspondence: vpinto@dei.uminho.pt (V.C.P.); gminas@dei.uminho.pt (G.M.)

Abstract: This paper presents the absorbance and fluorescence optical properties of various phytoplankton species, looking to achieve an accurate method to detect and identify a number of phytoplankton taxonomic groups. The methodology to select the excitation and detection wavelengths that results in superior identification of phytoplankton is reported. The macroscopic analyses and the implemented methodology are the base for designing a lab-on-a-chip device for a phytoplankton group identification, based on cell analysis with multi-wavelength lighting excitation, aiming for a cheap and portable platform. With such methodology in a lab-on-a-chip device, the analysis of the phytoplankton cells' optical properties, e.g., fluorescence, diffraction, absorption and reflection, will be possible. This device will offer, in the future, a platform for continuous, autonomous and in situ underwater measurements, in opposition to the conventional methodology. A proof-of-concept device with LED light excitation at 450 nm and a detection photodiode at 680 nm was fabricated. This device was able to quantify the concentration of the phytoplankton chlorophyll a. A lock-in amplifier electronic circuit was developed and integrated in a portable and low-cost sensor, featuring continuous, autonomous and in situ underwater measurements. This device has a detection limit of 0.01 µg/L of chlorophyll a, in a range up to 300 µg/L, with a linear voltage output with chlorophyll concentration.

Keywords: phytoplankton sensor; optical methods; photosynthetic pigment; lab-on-a-chip



Citation: Carvalho, D.A.M.; Pinto, V.C.; Sousa, P.J.; Magalhães, V.H.; Fernández, E.; Gomes, P.A.; Minas, G.; Gonçalves, L.M. Methodology for Phytoplankton Taxonomic Group Identification towards the Development of a Lab-on-a-Chip. *Appl. Sci.* **2022**, *12*, 5376. <https://doi.org/10.3390/app12115376>

Academic Editor: Francesco Dell'Olio

Received: 14 April 2022

Accepted: 24 May 2022

Published: 26 May 2022

Publisher's Note: MDPI stays neutral with regard to jurisdictional claims in published maps and institutional affiliations.



Copyright: © 2022 by the authors. Licensee MDPI, Basel, Switzerland. This article is an open access article distributed under the terms and conditions of the Creative Commons Attribution (CC BY) license (<https://creativecommons.org/licenses/by/4.0/>).

1. Introduction

Knowledge- and resilience-based management of marine ecosystem services is strongly required to cope with the pressures and impacts of the Anthropocene society [1]. To this aim, a constant and long-term monitoring of several environmental marine variables is needed to assess marine ecosystem health [2,3].

The study of phytoplankton species and their density estimation is a routine task in marine scientific research, since under certain conditions, the proliferation of algae can have a negative impact on the environment, fishing activities and the public health. This phenomenon is known as a harmful algal bloom (HAB) and can be as diverse as the species that originates it. For instance, blooms of high biomass of phytoplankton can drive the depletion of oxygen from the water, causing massive indiscriminate marine death. Another type of HAB consists of microalgae that, under certain conditions, are capable of producing toxins, and for some species, only a few hundreds of cells per litre is sufficient for the presence of toxins to be manifested in bivalves [4]. Other events are so massive that the

ocean colour blends with the pigment coloration of the species, and “red tides” can be observed [5]. Therefore, it is of extreme importance to study the population dynamics of phytoplankton communities [6], enabling knowledge about the potentially harmful algae present in aquatic marine systems. Local or regional authorities routinely perform this task by collecting phytoplankton and shellfish samples, analysing their toxicity and regulating the safe harvesting of seafood. The available methods for phytoplankton identification and quantification are based on optical and electronic microscopy, flow cytometry, image analysis, pigment analysis through high performance liquid chromatography (HPLC) and molecular methods [7,8]. However, these tasks can be expensive, time or reagent consuming, and require highly trained personnel, which can be limiting for in situ and real time HAB monitoring [9]. Efforts are being made to develop swift and precise measurement techniques for in situ automated measurements, such as FlowCAM, CytoBuoy, Imaging FlowCytobot or Laser Optical Plankton Counter [10,11], but these are bulky and very expensive (about EUR 26,000–130,000). Furthermore, these devices are mainly based on imaging methods which provide information about phytoplankton size, shape and cross-sectional area. However, to obtain precise taxonomic classification, advanced hardware and software and computer-assisted human experts are required to complement the complex data processing. Efforts for obtaining automated recognition of images using machine-learning techniques are in progress, but still have to be complemented with taxonomic expertise, which limit their in-situ application. A comparison of several optical and imaging methods already available and their operating capabilities can be found in [12].

Several photosynthetic pigments, such as chlorophylls a, b and c, carotenes, xanthophylls and phycobilins, are present in phytoplankton. Chlorophyll a is the main pigment of all organisms that performs photosynthesis with oxygen release, being widely used to estimate autotrophic phytoplankton biomass in aquatic ecosystems [13]. Distinct phytoplankton communities have specific marker pigments that can be used for taxonomic discrimination [14]. For instance, the main secondary pigment for most dinoflagellates is peridinin, while for diatoms fucoxanthin is the representative secondary pigment. These variations in pigment compositions produce different spectral characteristics across taxa that can be harnessed for phytoplankton identification [15]. The fluorometric methods are widely used for quantifying the photosynthetic pigments due their high sensitivity, high specificity and simplicity. However, most fluorometric system use expensive and bulky equipment and, mainly, cannot be applied for in situ detection. Some examples of these referenced devices are: the FluoroProbe II from bbe Moldaenke, which weighs 4.6 kg and costs around EUR 23,000; the Algae Online Monitor from Photon Systems Instruments, which weighs 3.4 kg and costs around EUR 12,990; and the AlgaeTorch from bbe Moldaenke, which weighs 1.2 kg and costs around EUR 7500 [16]. Therefore, development of new methodologies and novel devices, which can offer cost-effective, high-throughput and non-destructive analysis of microalgae species, has attracted increasing interest from research communities.

Recent works have reported on the development of portable sensors that measure different phytoplankton species through fluorescence detection of both the primary photosynthetic pigment (chlorophyll a) and accessory pigments (such as chlorophyll b, carotene, phycocyanin, phycoerythrin, and others) which are present in microalgae and cyanobacteria. Among these recently developed portable sensors, some can be highlighted, such as the development of a hand-held fluorescence sensor platform capable of selectively estimating green algae and cyanobacteria biomass [14]. In other works, the optofluidic detection systems are presented according to their category, such as fluorescence sensing, Raman spectroscopy and imaging flow cytometer, where they compare and discuss their advantages and disadvantages and identify avenues of further development of microfluidic systems for microalgal detection and characterization [17]. With an increasing demand for fluorescent portable sensors due to the benefits that fluorescent sensing technology offers, an overview of recent developments of portable fluorescence sensors can be found in [9,18]. However, most of them only differentiate different mixtures of green algae and

cyanobacteria, at a higher taxonomic group. In [19], the authors report a device featuring similar characteristics to the herein presented. However, despite its low cost and small dimensions, their device, as presented, is not a stand-alone system. In contrast, the system hereby presented aims to be integrated in a fully autonomous and portable lab-on-a-chip for in situ toxic phytoplankton quantification.

To our knowledge, there is not any methodology yet allowing the quantification and identification of phytoplankton groups at the same time, that also features low cost, portability, is prepared for continuous underwater monitoring and is autonomous. Therefore, we present an identification methodology for inclusion in a portable lab-on-a-chip, based on:

- (1) Multi-wavelength LED lighting excitation;
- (2) Photodiode based multi-wavelength fluorescence detection;
- (3) Scattering and absorption optical properties;
- (4) Single-cell analysis.

Phytoplankton has specific optical characteristics, which naturally absorbs light in the visible spectral range (mainly in blue light) and fluoresces in the 600 nm to 750 nm spectral range. Moreover, phytoplankton cells have different pigments, and each pigment has its own absorbance and fluorescence characteristics. Each phytoplankton group also have different cell sizes and complexity, which translates in different reflection, transmission and diffraction of light, as previously reported by flow cytometry [20]. Considering these optical properties, it is possible to identify and quantify the different groups of phytoplankton in aquatic systems [6]. Moreover, a single-cell analysis system is necessary to avoid the averaging effect when several cells are analysed at same time.

It should be noted that device miniaturization efforts emerged as a potential alternative, introducing improvements on efficiency, portability, automation, analysis time and reagents/samples reduction, as well as a reduction in costs [21].

In this work, the spectral characteristics of three species (*Nannochloropsis gaditana*, *Isochrysis galbana* and *Tetraselmis suecica*) were studied using benchtop flow cytometry, commercial spectrophotometers and fluorimeters. Knowing that phytoplankton pigments absorb and emit light at different wavelengths [2], excitation systems of multi-wavelength excitation (350–650 nm) and detection systems (550–750 nm) will be, in the future, implemented in the lab-on-a-chip, as a promising method to identify major phytoplankton groups in a high-resolution, portable (weight about 0.5 kg) and low-cost device (estimated cost of EUR 300). Despite being designed for identification of three species, this proposed lab-on-a-chip can be redesigned to detect other phytoplankton species by just specifying new absorption wavelengths and respective fluorescence signals as well as its morphological properties, foreseeing a future platform for improving the accuracy of phytoplankton quantification of in vivo samples.

2. Materials and Methods

2.1. Cultures

Three laboratory cultures of phytoplankton, representing six divisions (Table 1), were selected to be kept in culture and used for the various studies in this article. The initial cultures were provided by the Toralla Marine Science Station (ECIMAT), Vigo, Spain, from its Culture Collection of Algae and were periodically replicated to maintain stock. Each culture was maintained in 250 mL Erlenmeyer flasks and in an incubation chamber at a temperature of 18 °C (± 0.5 °C) and under illumination of fluorescent lamps with a 11 h light–13 h dark photoperiod. *Nannochloropsis gaditana*, *Isochrysis galbana* and *Tetraselmis suecica* were cultured in *Walne* medium prepared with seawater filtered through 0.2 μm pore size polycarbonate filters. Vitamins and soil extract were added to the filtered seawater. All culture mediums were sterilized in the autoclave and then stored in the refrigerator at 4 °C.

Table 1. Phytoplankton species in culture for the different studies.

Species	Family	Order	Class	Division
<i>Nannochloropsis gaditana</i>	Monodopsidaceae	Eustigmatales	Eustigmatophyceae	Ochrophyta
<i>Isochrysis galbana</i>	Isochrysidaceae	Isochrysidales	Coccolithophyceae	Haptophyta
<i>Tetraselmis suecica</i>	Chlorodendraceae	Chlorodendrales	Chlorodendrophyceae	Chlorophyta

Each of the phytoplankton species mentioned above have characteristics that allow them to be distinguished from each other, such as size, shape and characteristic pigments. Table 2 presents these characteristics for each of the species.

Table 2. Characteristics of each of the phytoplankton species.

Species	Size	Shape	Characteristic Secondary Pigments [15]
<i>Nannochloropsis gaditana</i>	3–5 μm	spherical	fucoxanthin
<i>Isochrysis galbana</i>	6–12 μm	ellipsoid	fucoxanthin and 19'-hexanoyloxyfucoxanthin
<i>Tetraselmis suecica</i>	10–15 μm	oval	chlorophyll-b

2.2. Apparatus Used for This Investigation

Commercial benchtop equipment was used to determine the optical and the morphological properties of the selected species. Absorption, fluorescence and single-cell flow cytometry were measured.

Absorption spectra of each phytoplankton species were recorded with a setup that includes a 170 W tungsten light source (Newport NRC 6334NS); a monochromator (Newport 74125); an optical fibre (Newport Standard Grade FS Fibre Optic), used to guide the light through the photodiode (Hamamatsu, S1336-5BQ); and a picoammeter (Keithley 487) to measure the photodiode current. Absorption spectra were scanned from 400 nm to 750 nm at 1 nm intervals.

Fluorescence spectra of species were acquired by a fluorimeter (Fluorolog of the brand HoribaJobin Yvon).

For the acquisition of different structural and functional parameters such as size (FS), relative complexity (SS) and fluorescent response (green (FL1), yellow (FL2), orange (FL3) and red (FL4)) of each of the phytoplankton species under study, a flow cytometer (COULTER® EPICS® XL-MCL™ Flow Cytometer, Beckman Coulter, Inc., Brea, California, USA) was used [22]. This flow cytometer uses a 488 nm excitation laser, directly measured in the forward scattering sensor. The side scattering (SS) sensor signal is separated using a 488 nm dichroic long-pass filter (488 DL) at a 45-degree angle to the light path (see Figure 1). This filter reflects the SS to the respective sensor but transmits fluorescent light of longer wavelengths. A 488 nm laser-blocking filter (488 BK) blocks any remaining laser light, transmitting only fluorescent light. The remaining optical filters separate the light for the four FL sensors. A 550 DL filter is at a 45-degree angle to the light path, and it reflects wavelengths lower than 550 nm to a 525 nm band-pass (525 BP) filter. In turn, this filter transmits light between 505 nm and 545 nm to the FL1 sensor. The 550 DL filter transmits between 555 nm and 725 nm to the next dichroic long-pass filter (600 DL), also positioned at a 45-degree angle to the light path, that reflects light between 555 nm and 600 nm to a 575 BP filter (560–590 nm) in front of the FL2 sensor. A dichroic long-pass filter, a 645 DL, reflects the light between 605 nm and 645 nm to a 620 BP filter (605–635 nm) in front of the FL3 sensor. The 645 DL filter also transmits light between 650 nm and 725 nm to a 675 BP filter (600–700 nm) in front of the FL4 sensor.

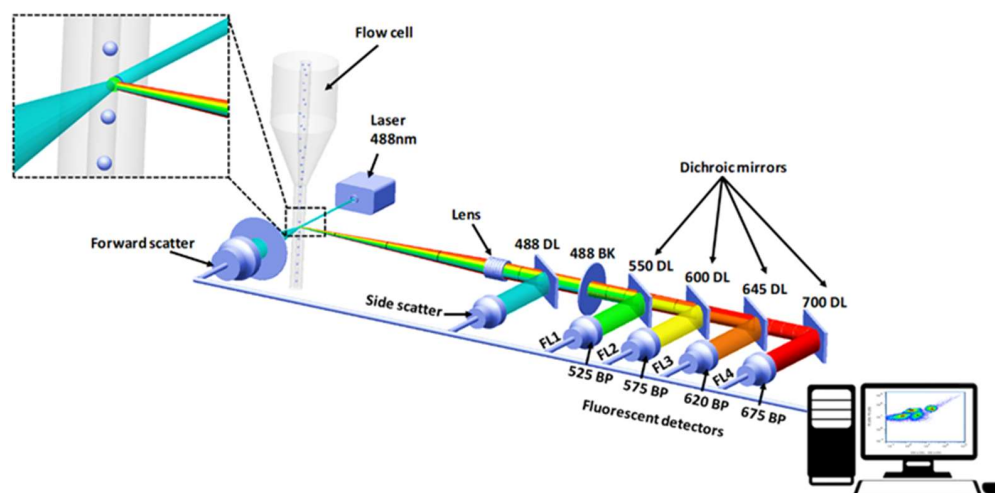


Figure 1. Filter configuration used in the commercial flow cytometer.

3. Characterization of Microalgae Optical Properties

The main objective of this study was to find optical properties that can be used to distinguish phytoplankton groups according to single characteristics. For that characterization, absorbance, fluorescence and flow cytometry were used as optical techniques. Absorption spectra (aiming for the colour of microalgae) is analysed in Section 4.1. Fluorescence in the range of 600 nm to 750 nm, with excitation in the range of 320 nm to 700 nm, is presented in Section 4.2. A 2–3 mL volume of culture with several cells from the same species was used in both characterization methodologies. Flow cytometry was also used once; in contrast with fluorometric tests where a group of cells (2–3 mL of seawater) were analysed together, in flow cytometry each cell is analysed individually. Single-cell analysis facilitates identification, avoiding the mean value (fluorescence, absorption or other property) obtained when several different species are presented in the same sample.

In this technique, the cells flow through a constriction channel in which they are illuminated with a 488 nm laser light, as described in Section 2. Forward light intensity (FS) is related to the size of the cell and 90° dispersion light intensity (SS) is related to the complexity of the cell (shape and external structure of the cell). Fluorescence is also measured at four fixed wavelengths, green, yellow, orange and red (FL1, FL2, FL3 and FL4, respectively), as described in Section 2.2. Single-cell analysis regarding forward scattering, side scattering and fluorescence in four wavelengths, using flow cytometry, is presented in Section 4.3. In order to ensure that the concentrations of each species are at the same level, the chlorophyll concentration present in each *in vivo* sample was measured. All the samples were collected in the stationary phase of growth and diluted to a similar chlorophyll concentration of ~250 µg/L.

4. Results and Discussions

4.1. Absorption Spectra

Figure 2 presents the absorbance spectra of each of the studied phytoplankton species. It is possible to observe that the absorbance has two peaks, one at 436 nm and the second one at 675 nm. In order to avoid differences in absorption that arise from different concentration of each species, the results presented in Figure 2 are normalized at 436 nm (absorbance spectra of all species to the same value at this wavelength, i.e., *Nannochloropsis gaditana* and *Tetraselmis suecica* spectrum values were multiplied by scale factors in such a way that their absorption at 436 nm has the same value as that of *Isochrysis galbana*) to allow the comparison of the absorbance spectra.

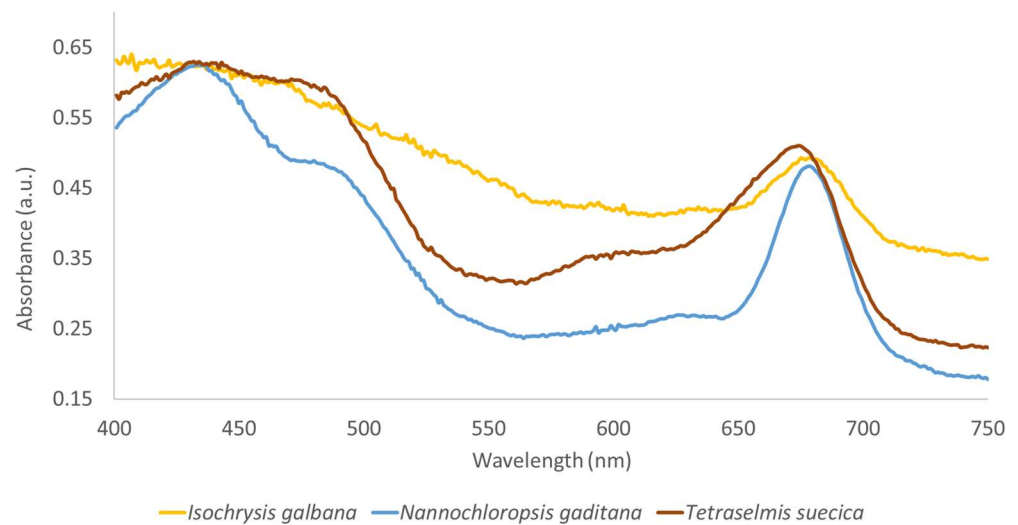


Figure 2. Relative absorbance spectrum of each studied phytoplankton species. All curves were normalized to the same absorbance value at 436 nm. The maximum standard deviation ($n = 3$) of 2% was obtained.

The absorption spectra corresponding to green algae (*Nannochloropsis gaditana* and *Tetraselmis suecica*; blue and brown lines in Figure 2) are very similar. The brown algae *Isochrysis galbana* (yellow line) showed a distinct absorption spectrum as compared with the other species under study.

Due to the scale normalization, to use the absorbance as an identification criterion, the ratio between the absorbance at two wavelengths must be used to avoid the effect of different concentrations. Table 3 presents the relation between the absorption coefficient at 530 nm and 436 nm. The results of this study show that although phytoplankton species can be grouped by colour by analysing their absorption spectra, the observed differences were not sufficient to allow differentiation, especially when more species were considered.

Table 3. Relationship between absorption at 530 nm and 436 nm for the phytoplankton species studied.

Species	A_{530}/A_{436}
<i>Nannochloropsis gaditana</i>	0.46
<i>Isochrysis galbana</i>	0.80
<i>Tetraselmis suecica</i>	0.56

4.2. Excitation/Fluorescence Spectrum Matrix

Fluorometric measurements, using the commercial fluorimeter described in Section 2.2, were performed for each species. Excitation was scanned from 400 nm to 650 nm (steps of 20 nm) and emission scanned from 400 nm to 850 nm (steps of 1 nm) for each excitation wavelength. Fluorescence at the same wavelength of the excitation was removed, since it results mainly from dispersion. Here, 2–3 mL of monocultures was analysed.

Figure 3 presents the fluorescence spectra (emission) of three of the presented phytoplankton species (*Nannochloropsis gaditana* (A), *Isochrysis galbana* (B) and *Tetraselmis suecica* (C)) for each excitation wavelength. Fluorescence values were normalized to the maximum value measured in the spectrum of each studied species.

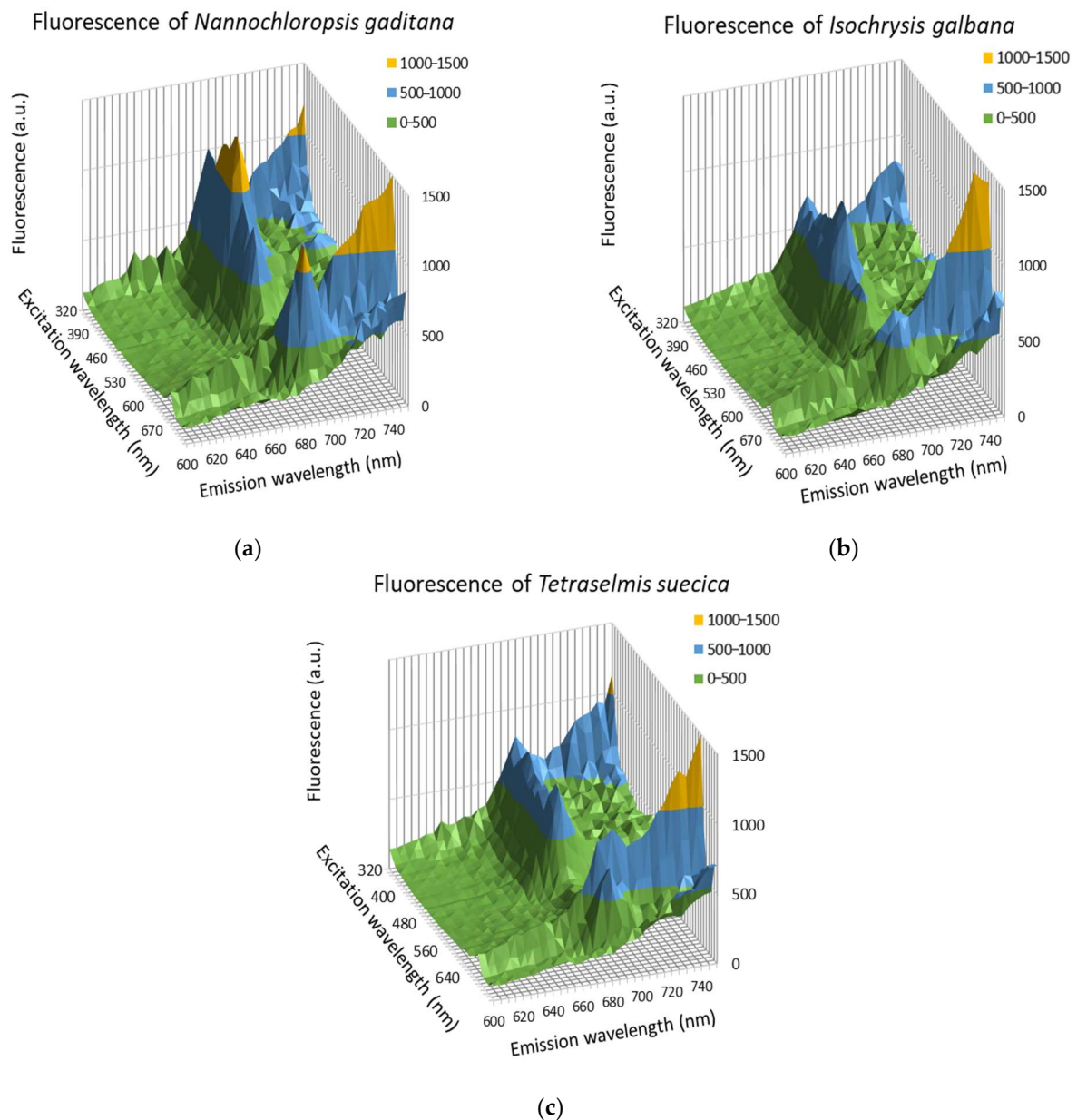


Figure 3. Fluorescence spectrum with excitation light scanned from 320 nm to 700 nm of (a) of *Nannochloropsis gaditana*, (b) *Isochrysis galbana* and (c) *Tetraselmis suecica*.

The three species show a fluorescence peak at 685 nm, for several excitation wavelengths. This peak corresponds to the fluorescence emission of chlorophyll a.

We then tried to find patterns in Figure 3 that are unique for each species. To this aim, we calculated the mean and standard deviation (σ), corresponding to the excitation/emission values for the three species using Equation (1), where F_{xy} is the fluorescence at each pair of excitation (x) and fluorescence (y) wavelengths, and \bar{F}_{xy} is the mean value from the three species.

$$\sigma_{xy} = \frac{\sqrt{\frac{\sum_1^3 (F_{xy} - \bar{F}_{xy})^2}{3}}}{\bar{F}_{xy}}, \tag{1}$$

Standard deviation between fluorescence in each excitation/emission wavelength from the three species is plotted in Figure 4. As depicted by Equation (1) of the standard deviation (σ_{xy}), a higher standard deviation means that the three species have different values of fluorescence (measured at wavelength represented in index y and when excited

at wavelength represented by index x). When the standard deviation has a value near zero, it means that all three species have equivalent fluorescence at that wavelength. The standard deviation is therefore used to understand which wavelengths can be used to better distinguish between species. The standard deviation of fluorescence for each pair of excitation/emission is higher when differences are found between the three species. Four main regions were found where standard deviation showed high (>30%) values (Figure 4). The respective excitation and emission wavelengths are presented in Table 4.

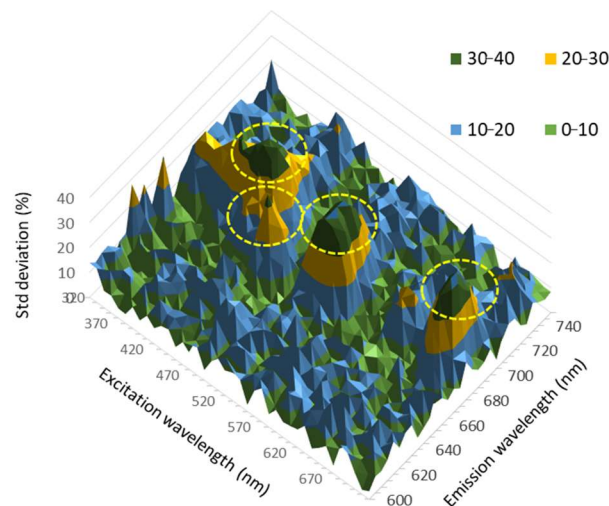


Figure 4. Standard deviation of the excitation/emission fluorescence values corresponding to *Nannochloropsis gaditana*, *Isochrysis galbana* and *Tetraselmis suecica*, calculated with Equation (1). The peaks represent the excitation/emission pairs where fluorescence differs in these three species. Excitation and emission wavelengths are plotted in horizontal axis and standard deviation (as percentage of mean value) in vertical axis.

Table 4. Pairs of excitation/emission wavelengths where difference between fluorescence of spectrum is higher, using the standard deviation as selection criteria.

Excitation (nm)	Emission (nm)	Standard Deviation (%)
420	685	39
450	670	33
530	680	47
680	680	39

The last region (excitation and emission at 680 nm) results from dispersion, since the same wavelength is used for excitation and emission and will not be considered for species differentiation. Emission in the 640 nm regions is almost equal in all species, at all excitation wavelengths (Figure 4). Figures 5 and 6 plot only these selected wavelengths, for the three species. Figure 5 represents fluorescence at 640 nm and 685 nm, when excitation is scanned from 320 nm to 700 nm, and Figure 6 shows the fluorescence emission spectrum, for excitation at 420 nm, 450 nm and 530 nm.

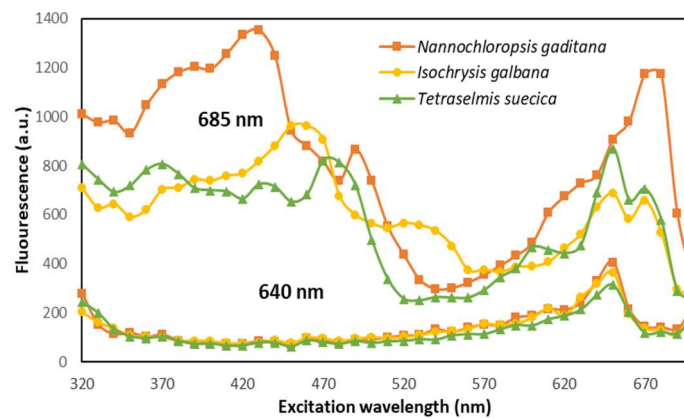


Figure 5. Fluorescence at 685 nm and 640 nm, when excitation is scanned from 320 nm to 700 nm. The maximum standard deviation ($n = 3$) of 5% was obtained.

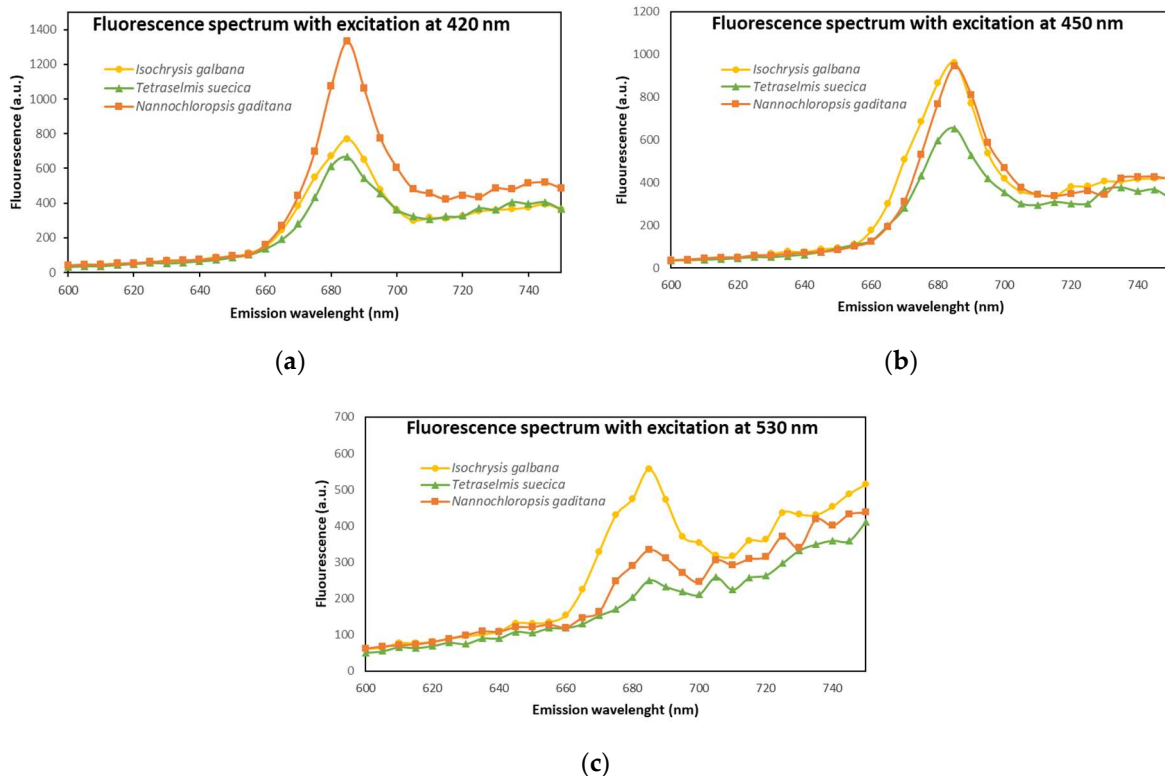


Figure 6. Fluorescence spectrum with excitation at: (a) 420 nm; (b) 450 nm; (c) 530 nm. The maximum standard deviation ($n = 3$) of 5% was obtained.

Differences between the species could be detected from Figures 5 and 6. As expected, the higher standard deviations from Table 4 are confirmed in the observed differences of the fluorescence spectra in Figures 5 and 6. We also identified the emission wavelengths where fluorescence is very similar for the studied species, which resulted to be emission wavelengths below 660 nm and emission wavelengths above 710 nm. These emission wavelengths can be used as reference.

Based on this study, excitation wavelengths of 420 nm, 450 nm and 530 nm and emission wavelengths of 640 nm and 685 nm were chosen as the most suitable to distinguish between these species. In order to confirm if the classification method could be used to discriminate potentially toxic species, the fluorescence spectrum of *Alexandrium tamarense* reported in [23,24] was used. Figure 7 shows the *Alexandrium tamarense* fluorescence

spectrum at 685 nm, when excitation light is scanned from 200 nm to 600 nm. The pairs of excitation/emission are presented in Table 5.

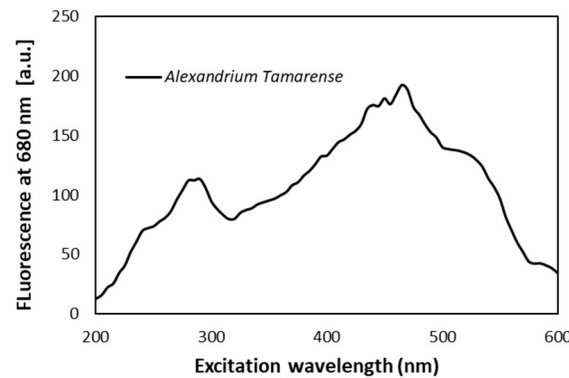


Figure 7. *Alexandrium tamarense* fluorescence spectrum with several excitation wavelengths. Reprinted/adapted with permission from Ref. [23]. Copyright © 2005 Elsevier B.V.

Table 5. Pairs of excitation/emission wavelengths used to distinguish *Nannochloropsis gaditana*, *Isochrysis galbana*, *Tetraselmis suecica* and *Alexandrium tamarense* and respective measured fluorescence value.

Fluorescence of <i>Nannochloropsis gaditana</i> (a.u.)		Emission (nm)	
Excitation (nm)		X: 685	Y: 640
A: 320		1010	
B: 420		1332	74
C: 450		944	71
D: 530		335	109
Fluorescence of <i>Isochrysis galbana</i> (a.u.)		Emission (nm)	
Excitation (nm)		X: 685	Y: 640
A: 320		707	
B: 420		768	74
C: 450		962	75
D: 530		533	110
Fluorescence of <i>Tetraselmis suecica</i> (a.u.)		Emission (nm)	
Excitation (nm)		X: 685	Y: 640
A: 320		805	
B: 420		665	66
C: 450		653	62
D: 530		251	90
Fluorescence of <i>Alexandrium tamarense</i> (a.u.)		Emission (nm)	
Excitation (nm)		X: 685	Y: 640
A: 320		79.84	
B: 420		150.4	8
C: 450		180.8	10
D: 530		128.8	9

For each species, nine ratios were derived from the fluorescence values shown in Table 5: six ratios resulting from the four fluorescence values obtained at 685 nm, with the four different excitation wavelengths (320 nm, 420 nm, 450 nm and 530 nm), named FBX/CX, FBX/DX, FBX/AX, FCX/DX, FCX/AX and FDX/AX; and three ratios between the emission obtained at 685 nm and 640 nm, for each excitation wavelengths (320 nm, 420 nm, 450 nm and 530 nm), named FBX/BY, FCX/CY and FDX/DY. These ratios are presented in Table 6 for each species.

Table 6. Fluorescence ratios used to distinguish *Nannochloropsis gaditana*, *Isochrysis galbana*, *Tetraselmis suecica* and *Alexandrium tamarense*.

Ratio	Specie			
	<i>Nannochloropsis gaditana</i>	<i>Isochrysis galbana</i>	<i>Tetraselmis suecica</i>	<i>Alexandrium tamarense</i>
F _{BX} /C _X	1.41 (M)	0.80 (m)	1.02	0.83
F _{BX} /D _X	3.98 (M)	1.44	2.65	1.17 (m)
F _{BX} /A _X	1.32	1.09	0.83 (m)	1.88 (M)
F _{CX} /D _X	2.82 (M)	1.80	2.60	1.40 (m)
F _{CX} /A _X	0.93	1.36	0.81 (m)	2.26 (M)
F _{DX} /A _X	0.33	0.75	0.31 (m)	1.61 (M)
F _{BX} /B _Y	18	10.35	10.08 (m)	18.80 (M)
F _{CX} /C _Y	13.30	12.83	10.53 (m)	18.08 (M)
F _{DX} /D _Y	3.07	4.85	2.79 (m)	14.31 (M)

For each ratio, the maximum (M) and minimum (m) values (maximum and minimum at each row) were selected. These maximum and minimum values of the fluorescence ratios were then used as identifying characteristics of each species. For each species, an identifier was calculated (GAD, GAL, SUE and TAM on Equation (2)). Maximum ratios from Table 6 are in the numerator and minimum ratios in the denominator of equations to calculate GAD, GAL, SUE and TAM (Equation (2)), but other ratios were also added to improve selectivity. A coefficient was also used to normalize all identifiers to a maximum value of 1 (1/284.6, 1/0.24, 61.8 and 1/20,423 respectively).

$$\begin{aligned}
 GAD &= \frac{F_{BX/CX} \times F_{BX/DX} \times F_{CX/DX} \times F_{BX/BY}}{284.6}, \\
 GAL &= \frac{F_{CX/CY} \times F_{BX/AX}}{0.24 \times F_{BX/CX} \times F_{BX/DX} \times F_{BX/BY} \times F_{DX/DY}}, \\
 SUE &= \frac{61.8}{F_{BX/AX} \times F_{CX/AX} \times F_{DX/AX} \times F_{BX/BY} \times F_{CX/CY} \times F_{DX/DY}}, \\
 TAM &= \frac{F_{BX/AX} \times F_{CX/AX} \times F_{DX/AX} \times F_{BX/BY} \times F_{CX/CY} \times F_{DX/DY}}{20423 \times F_{BX/DX} \times F_{CX/DX}},
 \end{aligned}
 \tag{2}$$

Validation of the equations was made by calculating the four identifiers (Equation (2)) with the fluorescence values of the four species (Table 6), resulting in the values in Table 7.

Table 7. Four identifiers (GAD, GAL, SUE and TAM) calculated from fluorescence ratios of the three species.

Species	GAD	GAL	SUE	TAM
<i>Nannochloropsis gaditana</i>	1.00	0.08	0.25	0.09
<i>Isochrysis galbana</i>	0.24	1.00	0.48	0.54
<i>Tetraselmis suecica</i>	0.21	0.09	1.00	0.00
<i>Alexandrium tamarense</i>	0.00	0.01	0.00	1.00

The species *Nannochloropsis gaditana* and *Isochrysis galbana* are clearly identified from the calculated identifier GAD and GAL, respectively. The identifier GAD showed the highest value (1.00) when *Nannochloropsis gaditana* is present, whereas this identifier has low values (0.24, 0.21 and 0.00) when calculated with the fluorescence measurements of the three other species.

The identifier GAL has the highest value (1.00) with the fluorescence of *Isochrysis Galbana*, but very small values (0.08, 0.09 and 0.01) when calculated from the fluorescence measurements corresponding to the three other species.

In addition, the species *Tetraselmis suecica* can be identified, but with less confidence than the previous species. The identifier SUE has the value 1.00 when calculated with the

fluorescence of species *Tetraselmis suecica*, and values below 0.48 when calculated with the fluorescence measurements from the other species.

The toxic species (*Alexandrium Tamarense*) can be clearly identified from *Nannochloropsis gaditana* and *Tetraselmis suecica*. However, TAM showed a value of 0.54 in the presence of *Isochrysis galbana*, a value that still allows its identification, but with less confidence.

An identifying algorithm should calculate the value of the four identifiers (GAL, GAD, SUE and TAM), and the higher value obtained in these four identifiers reveals the presented species.

If more different species are presented for identification, the same methodology can be used. However, more emission ratios (than the ones presented in Table 6) should be used in order to improve selectivity of the identification process.

We were, therefore, able to identify phytoplankton taxonomic groups using a commercial fluorimeter, thus allowing to fulfil the objective of this work: to develop a lab-on-a-chip sensor capable of distinguishing toxic and non-toxic phytoplankton species through the analysis of fluorescence spectrum and intensity at several excitation wavelengths.

4.3. Single-Cell Analysis

4.3.1. Study of Size versus Complexity

Figure 8 reports on the size versus complexity for each of the selected phytoplankton species, measured with the flow cytometer. The forward scatter (FS in y-axis of Figure 8) represents the size of the cell, and the side scatter (SS in x-axis) is the granularity and complexity of the cell.

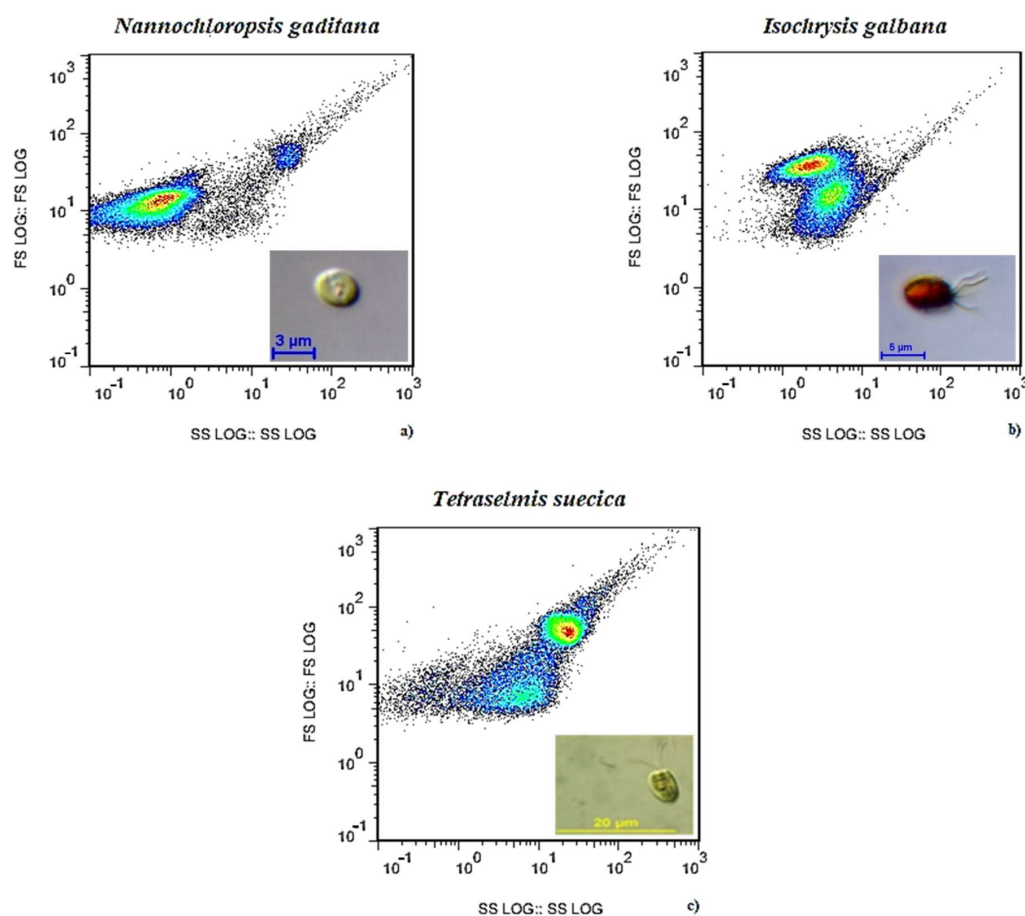


Figure 8. Size as a function of complexity for each of the phytoplankton species, obtained by flow cytometry: (a) *Nannochloropsis gaditana*; (b) *Isochrysis galbana*; (c) *Tetraselmis suecica*.

As expected, each species presents different results in terms of size and complexity (Figure 8). *Nannochloropsis gaditana* (Figure 8a) is the smallest (FS) and least complex (SS)

species studied, followed by the *Isochrysis galbana* (Figure 8b), which is a little larger and more complex.

Tetraselmis suecica (Figure 8c) shows large and complex cells. When all the species are mixed, the results from Figure 9 can be expected, where differentiation and similarities between species can be better visualized. Moreover, the discrimination of toxic phytoplankton species by the flow cytometry method was clearly validated in [25]. The cytometry results have revealed excellent capabilities for rapid and automatic detection of several cells of phytoplankton within a flux, simultaneously analysing several optical parameters. Thus, a solution based on lab-on-a-chip flow cytometry could revolutionize the paradigm of portable and autonomous strategies for in situ phytoplankton quantification and species determination, as designed in Section 5.

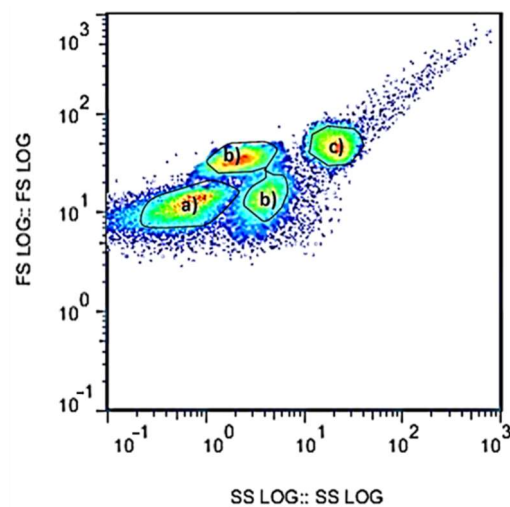


Figure 9. Cytometry results from individual species in the same graph: (a) *Nannochloropsis gaditana*; (b) *Isochrysis galbana*; (c) *Tetraselmis suecica*.

4.3.2. Study of Fluorescence in Four Wavelengths of the Visible Spectrum

Figure 10 represents the relative fluorescence for each of the phytoplankton species in four wavelengths of the visible spectrum: green (FL1-525 nm) (Figure 10a), yellow (FL2-575 nm) (Figure 10b), orange (FL3-620 nm) (Figure 10c) and red (FL4-675 nm) (Figure 10d), obtained with the flow cytometer, using a laser excitation at 488 nm.

Nearly 3000 cells were analysed in each test. Counts in the y-axis represent the number of cells for each intensity range in the x-axis. The intensity of fluorescence in these species is clearly different when considering the FL1, FL3 and FL4 histograms. Regarding the FL2 histogram, almost all the studied species show the same histogram.

FL4 can be used as the base histogram to distinguish cells. FL4 fluorescence intensities (600–700 nm) are almost an order of magnitude different in *Nannochloropsis gaditana* and *Tetraselmis suecica* (1 and 40, respectively) as depicted by Figure 10d. This difference could be attributed to the different chlorophyll cellular content characteristic of each species.

A lab-on-a-chip that measures fluorescence in these four wavelengths (FL1-525 nm, FL2-575 nm, FL3-620 nm and FL4-675 nm) can be used to distinguish between these species, except those from the same group. Complementing the lab-on-a-chip with forward scattering and side scattering, further differentiation is also possible.

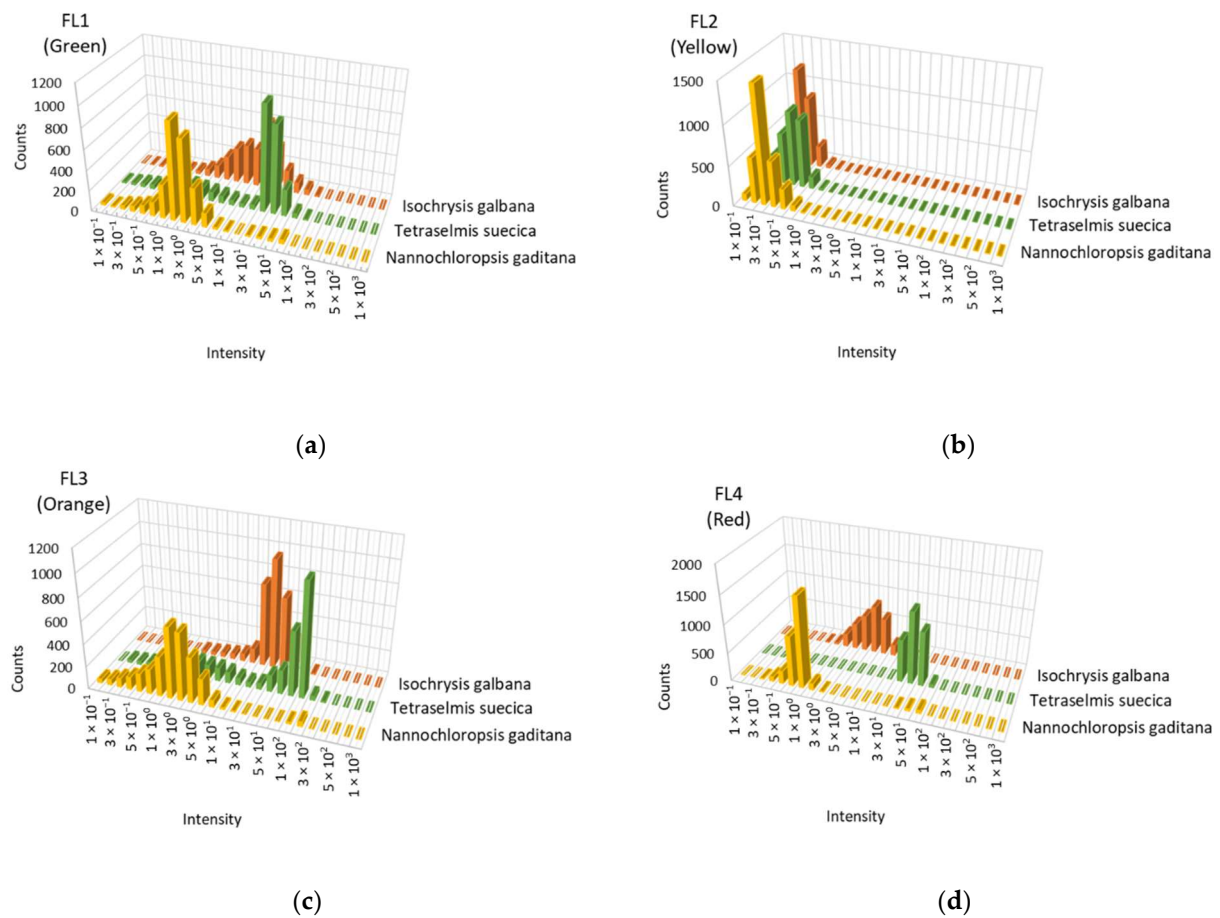


Figure 10. Size as a function of complexity for each of the phytoplankton species, obtained by flow cytometry: (a) FL1–525 nm (green); (b) FL2–575 nm (yellow); (c) FL3–620 nm (orange); (d) FL4–675 nm (red).

4.4. Preliminary Tests of Chlorophyll a Measurements

With the propose of evaluation, validation and output of the electronic features and measuring principles presented in this paper, a simple and portable device was fabricated, using excitation at 450 nm and detection at 680 nm. The fabricated device has only one excitation wavelength (450 nm) and one fluorescence wavelength (680 nm). The analysis was performed in a 1 cm^3 volume. This device was used to measure chlorophyll a content of cells.

4.4.1. Fabricated Device

The portable and low-cost fluorescent detection system was fabricated using four subsystems: (1) the illumination system containing two commercial LEDs with maximum emission peak centered at 450 nm; (2) the photodetection system containing a low-noise and high-quantum-efficiency photodiode with a 680 nm optical bandpass filter for supressing the excitation signal at 450 nm and improving the sensitivity by drastically reducing the background noise; (3) the power source batteries; and (4) the electronics system for readout and control, as described in Section 4.4.2.

The optical–electronic system was assembled in a 90° configuration using a 3D printed support ensuring the correct alignment and position of the optical components. It was designed with dimensions suitable for analysis in standard cuvettes. At this early stage of development, the control and readout electronics were soldered in a PCB placed externally to the assembled device (Figure 11).

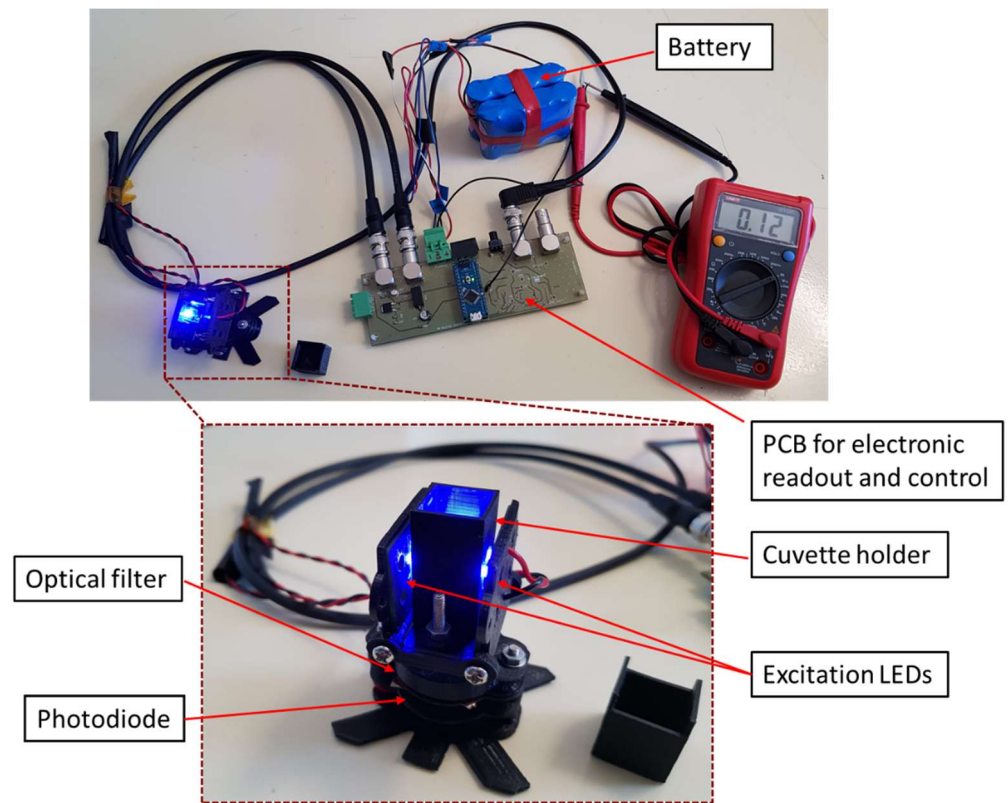


Figure 11. Photograph of the developed device showing the several subsystems.

4.4.2. Readout Electronics

The major problem associated with the fluorescence signal is its low amplitude and, consequently, low current in the photodiodes (tens of nA were measured for low chlorophyll concentrations), so it is easily affected by surrounding noise. The implementation of a high-sensitivity, noise-free reading circuit capable of making viable readings is required. This mechanism can be implemented using synchronous detectors as the lock-in amplifier, which extracts the signal embedded in noise, allowing a higher signal-to-noise ratio, since noise decreases as frequency increases [26]. Shifting the useful detection signal to higher frequencies, the signal-to-noise ratio is increased, allowing the detection of smaller frequency signals, such as those expected from phytoplankton fluorescence, by modulating the excitation light (LED). The simplest approach for modulating the LED is to pulse it in the order of kHz, shifting the signal of interest to frequencies where lower noise is expected. The original DC signal (from fluorescence) is recovered through a synchronous demodulator that will shift the signal from the modulation frequency to DC, attenuating all signals that are not synchronized with excitation reference.

The representative block diagram of a lock-in amplifier is shown in Figure 12.

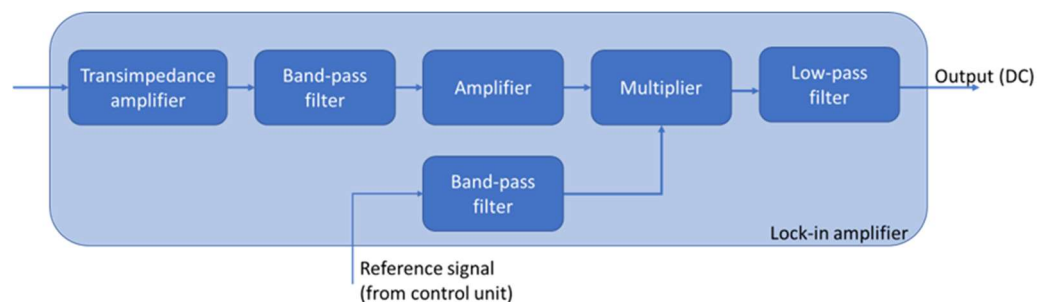


Figure 12. Lock-in amplifier functional block diagram.

4.4.3. Performance Testing and Calibration

The performance of the proposed device was determined considering the measurement range, limit of detection and linearity. As such, an initial calibration was performed using standard solutions of chlorophyll a (from spinach, Sigma-Aldrich C5753-1 mg) dissolved in acetone 90%. Several dilutions of this standard solution were carried out with known concentrations in the range of 0.01–300 $\mu\text{g/L}$ (Figure 13). As it can be seen from the presented results, the sensor exhibits a linear response ($R^2 = 0.9963$) with a 0.01 $\mu\text{g/L}$ detection limit.

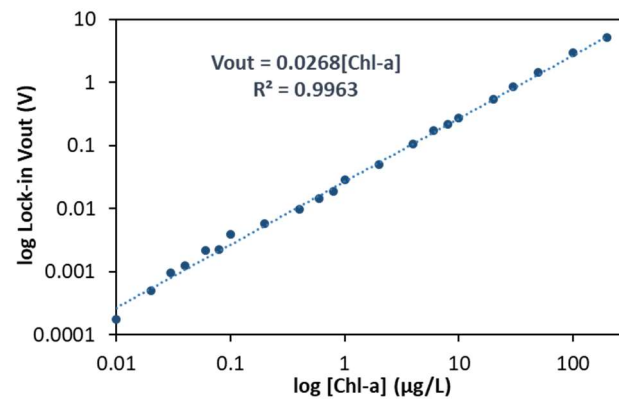


Figure 13. Calibration curve of the sensor using chlorophyll a standard solutions.

Experimental tests were also performed in the device with collected seawater. Water samples were diluted (with filtered seawater) to obtain five different water samples with chlorophyll a concentration in the range 0.05–2 $\mu\text{g/L}$. This low concentration allowed assessing the limit of detection of the device using natural seawater samples (Figure 14). These measurements showed an excellent performance for outputting the chlorophyll a concentrations, from 0.05 to up to 300 $\mu\text{g/L}$, with in vivo phytoplankton, allowing to conclude the viability of the developed electronics illumination and readout circuits.

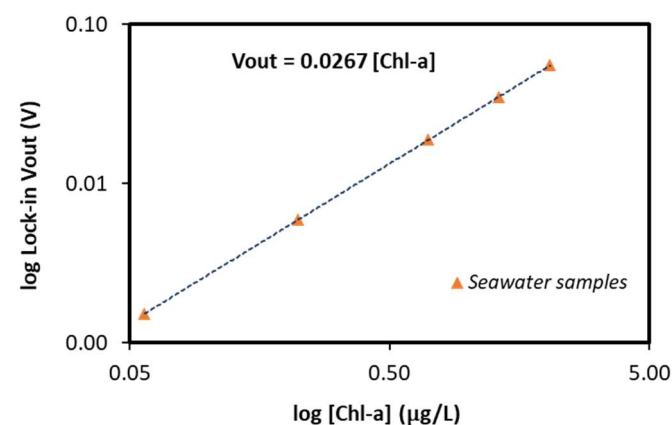


Figure 14. Measurement of five diluted seawater samples, with chlorophyll a concentration in the range 0.05–2 $\mu\text{g/L}$.

5. Towards the Development of a Lab-on-a-Chip

After the previous validation of the wavelengths, a lab-on-a-chip device for phytoplankton group identification was designed, resorting to the spectral characteristics of each of the species used in this study. The algorithm from Section 4.2 requires four excitation wavelengths (320 nm, 420 nm, 450 nm and 530 nm) that can be obtained with LEDs or lasers, and two detection wavelengths (640 nm and 685 nm) with respective optical filters. The methodology described in Section 2.2 requires only one excitation wavelength, but the detection needs six photodetectors with optical filters for the six wavelengths. Furthermore,

the proposed lab-on-a-chip will comprise a constriction channel, in order to analyse single cells (or a few cells) to avoid measurement of mean values of optical properties that results from larger volumes with several different cells. This allows the phytoplankton cells to move in a single centre line and pass, one by one, through the detection area.

The schematic representation of the lab-on-a-chip is shown in Figure 15. This device has integrated fluorescence and scattering detection. It comprises a microfluidic die, which includes microchannels and a detection chamber; a set of excitation light sources with wavelengths specific for the different species of phytoplankton; CMOS silicon photodiodes; signal amplifiers; data acquisition and processing; and a microcontroller. All of these parts are integrated in a portable and compact platform.

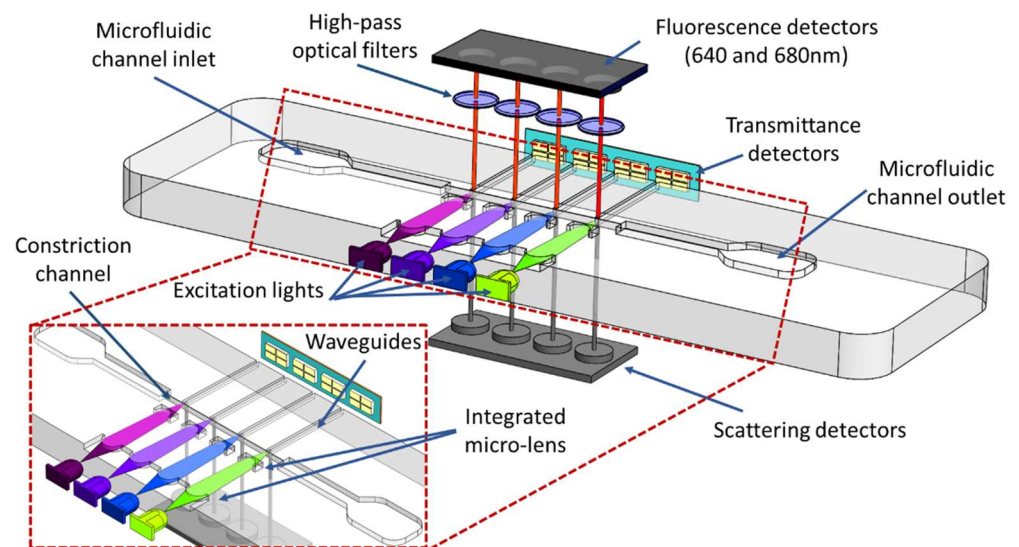


Figure 15. Schematic illustration of the lab-on-a-chip for phytoplankton group identification and quantification based on fluorescence detection.

5.1. Microfluidic Die

The microfluidic die was designed to deliver the phytoplankton cells to the detection channel. A sheath flow could be used to confine the sample cells to a focus point where the morphology features (scattering sensor), absorbance (transmittance detectors) and fluorescence (fluorescence detectors) can be measured for phytoplankton classification. This microfluidic die is fabricated in polydimethylsiloxane (PDMS) due to its flexibility, biocompatibility and optical transparency in the visible/ultra-violet (down to 230 nm) spectral range, which allows the use of optical detection methods. The fabrication of the PDMS microfluidic die is a simple and low-cost method, without the need of cleanroom facilities, where it was cast with an SU-8 mould (soft lithography) obtained by a high-resolution photolithography process. The detailed processing steps for the SU-8 mould fabrication can be found in [27].

5.2. Optical Detection System

Based on the results obtained in Section 4, four micro-LEDs were chosen as the excitation light source, with wavelengths of 320, 420, 450 and 530 nm. Lenses could be fabricated in the PDMS die in order to focus light on a small spot located in the constriction channel. Two photodetectors (with band-pass filters at 640 nm and 680 nm) are placed at a 90° angle with respect to the LEDs to measure fluorescence and minimize the influence of excitation light (see Figure 15). Forward (FS) and lateral (SS) detection can also be implemented. Transmitted light can be measured by means of photodetectors added in front of each excitation light (LEDs or laser). Waveguides could be used to conduct the transmitted light (FS) from the cell to the photodetector. The bottom photodiodes can be used to measure cell complexity (SS) at the excitation wavelength. The control and readout

electronics are based on a lock-in amplifier, as described and validated in Sections 4.4.2 and 4.4.3, respectively.

6. Conclusions

This paper presents the features of absorbance and fluorescence optical properties of three phytoplankton species, and it serves as a preliminary step towards the development of a portable and low-cost lab-on-a-chip capable of identifying phytoplankton taxonomic groups. A methodology for the selection of suitable excitation/emission pairs in fluorimetry analyses is also described. Based on this methodology, a lab-on-a-chip device is proposed that is able to distinguish between four phytoplankton species (one of them, *Alexandrium tamarense*, known for being toxic), using excitation at 320 nm, 430 nm, 450 nm and 530 nm and detection at 640 nm and 680 nm wavelengths. The measurement principle and electronics were validated (with excitation at 450 nm and fluorescent emission at 680 nm wavelengths). The developed device was able to estimate phytoplankton biomass from in vivo chlorophyll a, with concentrations ranging from 0.01 to 300 µg/L. The detection limit of the proposed device was measured as 0.01 µg/L for chlorophyll a standard solutions, and as 0.05 µg/L for in vivo measurements. Further work will focus on the integration of the several excitation and emission wavelengths in a single lab-on-a-chip device for multi-species identification, paying special attention to the identification of toxic species in the presence of other non-toxic species. This device exhibits great potential for oceanographic research, since it allows in vivo analysis with less work time and without the need for complex extraction procedures. Furthermore, the proposed low-cost technology (<300 EUR) will allow future massive deployments of those sensors, enabling a better understanding of the ocean, with systematic measures and analyses of potentially toxic (and non-toxic) phytoplankton.

7. Patents

A European Patent Application resulting from the work reported in this manuscript was submitted with EP number EP3943918A1 and title: “Device for identification and quantification of phytoplankton, methods and uses thereof”.

Author Contributions: Conceptualization, D.A.M.C., V.C.P., P.J.S., E.F., G.M. and L.M.G.; Funding acquisition, G.M. and L.M.G.; Methodology, D.A.M.C., V.C.P., P.J.S., V.H.M., G.M. and L.M.G.; Supervision, E.F., G.M. and L.M.G.; Writing—original draft, D.A.M.C., V.C.P. and P.J.S.; Writing—review and editing, E.F., P.A.G., G.M. and L.M.G. All authors have read and agreed to the published version of the manuscript.

Funding: This work was co-financed by the European Regional Development Fund (ERDF) through the Interreg VA Spain-Portugal (POCTEP) 2014–2020 Program under grant agreement 0591_FOOD-SENS_1_E, under the national support to R&D units grant, through the reference project UIDB/04436/2020 and UIDP/04436/2020, and by project NORTE-08-5369-FSE-000039 co-founded by the European Social Fund FSE and through National funds NORTE 2020 and Regional Operacional Programa of North 2014/2020. The University of Vigo work was funded by a Xunta de Galicia grant to the Biological Oceanography Research Group (Consolidación e estruturación de unidades). This output reflects only the views of the authors, and the program authorities cannot be held responsible for any use that may be made of the information contained therein.

Institutional Review Board Statement: Not applicable.

Informed Consent Statement: Not applicable.

Data Availability Statement: Not applicable.

Acknowledgments: D.C. thanks the NORTE 2020 for the BD/ Do*Mar/1017/2016 grant, V.M. thanks the FCT for the PD/BD/150581/2020 grant, V.P. thanks FCT for her contract funding provided through 2021.01087.CEECIND, and P.S. thanks FCT for his contract funding provided through 2021.01086.CEECIND.

Conflicts of Interest: The authors declare no conflict of interest.

References

1. Braat, L.C.; de Groot, R. The ecosystem services agenda: bridging the worlds of natural science and economics, conservation and development, and public and private policy. *Ecosyst. Serv.* **2012**, *1*, 4–15. [CrossRef]
2. Miloslavich, P.; Pearlman, J.; Kudela, R. Sustainable Observations of Plankton, the Sea's Food Foundation. *EOS* **2018**, *99*, 1–5. [CrossRef]
3. Pinto, V.C.; Faria, C.A.; Gomes, P.A.; Minas, G.; Gonçalves, L.M. Next Generation Coastal Monitoring Systems. In *Abstract Book, Proceedings of the Campus do Mar International Science Conference 2016, Oceans: Future Sustainability Challenges, Vila Real, Portugal, 17–18 November 2016*; Cabecinha, E., Queiroga, H., Moreira, H., Alencão, A., Monteiro, S.M., Coimbra, A.M., Eds.; University of Trás-os-Montes and Alto Douro (UTAD): Vila Real, Portugal, 2016; p. 144.
4. Reguera, B.; Escalera, L.; Pazos, Y.; Moroño, A. *Episodios de Fitoplancton Tóxico en la RÍA de Vigo; Una Aproximación Integral al Ecosistema Marino de la Ría de Vigo*; Instituto de Estudios Vigüeses: Vigo, Spain, 2008.
5. Lindsey, R.; Scott, M. What Are Phytoplankton? 2010. Available online: <https://earthobservatory.nasa.gov/features/Phytoplankton> (accessed on 5 September 2021).
6. Su, R.; Chen, X.; Wu, Z.; Yao, P.; Shi, X. Assessment of phytoplankton class abundance using fluorescence excitation-emission matrix by parallel factor analysis and nonnegative least squares. *Chin. J. Oceanol. Limnol.* **2015**, *33*, 878–889. [CrossRef]
7. Peperzak, L.; Zetsche, E.-M.; Gollasch, S.; Artigas, L.F.; Bonato, S.; Creach, V.; De Vré, P.; Dubelaar, G.B.; Henneghien, J.; Hess-Erga, O.-K.; et al. Comparing flow cytometry and microscopy in the quantification of vital aquatic organisms in ballast water. *J. Mar. Eng. Technol.* **2018**, *19*, 68–77. [CrossRef]
8. Karlson, B.; Artigas, F.; Créach, V.; Louchart, A.; Wacquet, G.; Seppala, J. *Novel Methods for Automated In Situ Observations of Phytoplankton Diversity*; WP3, D3.1, Version 9; IFREMER JERICO-NEXT: Brest, France, 2017; pp. 1–69. [CrossRef]
9. Silva, G.M.; Campos, D.F.; Brasil, J.A.T.; Tremblay, M.; Mendiondo, E.M.; Ghiglieno, F. Advances in Technological Research for Online and In Situ Water Quality Monitoring—A Review. *Sustainability* **2022**, *14*, 5059. [CrossRef]
10. Dunker, S.; Boho, D.; Wäldchen, J.; Mäder, P. Combining high-throughput imaging flow cytometry and deep learning for efficient species and life-cycle stage identification of phytoplankton. *BMC Ecol.* **2018**, *18*, 51. [CrossRef] [PubMed]
11. Göröcs, Z.; Tamamitsu, M.; Bianco, V.; Wolf, P.; Roy, S.; Shindo, K.; Yanny, K.; Wu, Y.; Koydemir, H.C.; Rivenson, Y.; et al. A deep learning-enabled portable imaging flow cytometer for cost-effective, high-throughput, and label-free analysis of natural water samples. *Light. Sci. Appl.* **2018**, *7*, 66. [CrossRef] [PubMed]
12. Lombard, F.; Boss, E.; Waite, A.M.; Vogt, M.; Uitz, J.; Stemann, L.; Sosik, H.M.; Schulz, J.; Romagnan, J.-B.; Picheral, M.; et al. Globally Consistent Quantitative Observations of Planktonic Ecosystems. *Front. Mar. Sci.* **2019**, *6*, 196. [CrossRef]
13. Speer, B.R. Photosynthetic Pigments. University of California, Berkeley Museum of Paleontology. 1997. Available online: <http://www.ucmp.berkeley.edu/glossary/gloss3/pigments.html> (accessed on 8 September 2018).
14. Shin, Y.-H.; Barnett, J.Z.; Gutierrez-Wing, M.; Rusch, K.A.; Choi, J.-W. A hand-held fluorescent sensor platform for selectively estimating green algae and cyanobacteria biomass. *Sens. Actuators B Chem.* **2018**, *262*, 938–946. [CrossRef]
15. Zieger, S.E.; Seoane, S.; Laza-Martinez, A.; Knaus, A.; Mistlberger, G.; Klimant, I. Spectral Characterization of Eight Marine Phytoplankton Phyla and Assessing a Pigment-Based Taxonomic Discriminant Analysis for the in Situ Classification of Phytoplankton Blooms. *Environ. Sci. Technol.* **2018**, *52*, 14266–14274. [CrossRef] [PubMed]
16. Pires, M.D. *Evaluation of Fluorometers for the In Situ Monitoring of Chlorophyll and/or Cyanobacteria*; 1203593-0002010; Deltares: Delft, The Netherlands, 2010.
17. Zheng, X.; Duan, X.; Tu, X.; Jiang, S.; Song, C. The Fusion of Microfluidics and Optics for On-Chip Detection and Characterization of Microalgae. *Micromachines* **2021**, *12*, 1137. [CrossRef] [PubMed]
18. Shin, Y.-H.; Gutierrez-Wing, M.T.; Choi, J.-W. Review—Recent Progress in Portable Fluorescence Sensors. *J. Electrochem. Soc.* **2021**, *168*, 017502. [CrossRef]
19. Zieger, S.E.; Mistlberger, G.; Troi, L.; Lang, A.; Confalonieri, F.; Klimant, I. Compact and Low-Cost Fluorescence Based Flow-Through Analyzer for Early-Stage Classification of Potentially Toxic Algae and in Situ Semiquantification. *Environ. Sci. Technol.* **2018**, *52*, 7399–7408. [CrossRef] [PubMed]
20. Malkasian, A.; Nerini, D.; van Dijk, M.A.; Thyssen, M.; Mante, C.; Gregori, G. Functional analysis and classification of phytoplankton based on data from an automated flow cytometer. *Cytom. Part A* **2011**, *79A*, 263–275. [CrossRef] [PubMed]
21. Bange, A.; Halsall, H.B.; Heineman, W.R. Microfluidic immunosensor systems. *Biosens. Bioelectron.* **2005**, *20*, 2488–2503. [CrossRef] [PubMed]
22. Coulter, B. *COULTER® EPICS® XL™ Flow Cytometer COULTER® EPICS® XL-MCL™ Flow Cytometer SYSTEM II™ Software*; Beckman Coulter, Inc.: Brea, CA, USA, 2010.
23. Zhang, Q.-Q.; Lei, S.-H.; Wang, X.-L.; Wang, L.; Zhu, C.-J. Discrimination of phytoplankton classes using characteristic spectra of 3D fluorescence spectra. *Spectrochim. Acta Part A Mol. Biomol. Spectrosc.* **2006**, *63*, 361–369. [CrossRef] [PubMed]
24. Zhang, F.; He, J.; Su, R.; Wang, X. Assessing Phytoplankton Using a Two-Rank Database Based on Excitation-Emission Fluorescence Spectra. *Appl. Spectrosc.* **2011**, *65*, 1–9. [CrossRef] [PubMed]
25. Tran, D.; Haberkorn, H.; Soudant, P.; Ciret, P.; Massabuau, J.-C. Behavioral responses of *Crassostrea gigas* exposed to the harmful algae *Alexandrium minutum*. *Aquaculture* **2010**, *298*, 338–345. [CrossRef]

26. Orozco, L. Synchronous Detectors Facilitate Precision, Low-Level Measurements. *Analog. Dialogue* **2014**, *48*, 1–5.
27. Pinto, V.C.; Sousa, P.J.; Cardoso, V.F.; Minas, G. Optimized SU-8 Processing for Low-Cost Microstructures Fabrication without Cleanroom Facilities. *Micromachines* **2014**, *5*, 738–755. [[CrossRef](#)]